



**Grant Agreement No. 783169**  
**U-Geohaz – “Geohazard impact**  
**assessment for urban areas”**

## **Deliverable D3.5: Updated Deformation activity map (V2)**

**A deliverable of WP3: Early Warning System for Volcanic activity**

**Due date of deliverable:** 30/06/2019

**Actual submission date:** 06/08/2019

**Lead contractor for this deliverable: CTTC**

Dissemination Level		
PU	Public	
PP	Restricted to other programme participants (including the Commission Services)	
RE	Restricted to a group specified by the Consortium (including the Commission Services)	
CO	Confidential, only for members of the Consortium (including the Commission Services)	
TN	Technical Note, not a deliverable, only internal for members of the Consortium	x



European Union  
Civil Protection and  
Humanitarian Aid

## **Table of Content**

<b>EXECUTIVE SUMMARY .....</b>	<b>3</b>
<b>REFERENCE DOCUMENTS .....</b>	<b>4</b>
<b>1 INTRODUCTION .....</b>	<b>6</b>
<b>2 DATASET DESCRIPTION .....</b>	<b>6</b>
<b>3 PROCEDURE DESCRIPTION .....</b>	<b>7</b>
3.1 Phase splitting .....	8
3.2 DAM and ADA generation: High frequency path .....	9
3.2.1 Remarks on the used approach and issues to be solved .....	11
3.3 DIM generation: Low frequency path .....	11
<b>4 MAP DELIVERY FORMAT .....</b>	<b>13</b>
<b>5 OBTAINED RESULTS .....</b>	<b>14</b>
<b>6 OBSERVATIONS .....</b>	<b>15</b>
<b>7 REFERENCES .....</b>	<b>17</b>

## **EXECUTIVE SUMMARY**

This document contains the description of the procedure used to derive the deformation maps in the Canary Island test site and the obtained results over the Tenerife, Hierro and La Palma islands. These results have been obtained in the frame of the task "3.3 Deformation activity maps" of the work package 3 "Early Warning System for Volcanic activity" and represents the final version of the deliverable 3.5 "Updated Deformation activity map", led by CTTC.

The main goal of WP3 is to implement and test an early warning system based on the use of different geodetic techniques and on the exploitation of the deformation activity maps based on Sentinel-1 updated each 6-days. In particular, the goal of the task 3.3 aims is the generation of the deformation activity map (DAM) proposed in SAFETY in the Canary Islands test site with a 6-day temporal repeatability.

This deliverable is a technical report to describe the Deformation Activity maps obtained over the Tenerife, Hierro and La Palma islands and the used methodology. The final results are satisfactory. However, it has been tuned to the site requirements and some issues have to be solved in order to make it replicable to other sites.

**REFERENCE DOCUMENTS**

N°	Title
RD1	DoW Part B

## **CONTRIBUTORS**

Contributor(s)	Company	Contributor(s)	Company
Oriol Monserrat Hernandez	CTTC	Michele Crosetto	CTTC
Vrinda Krishnakumar	CTTC	Enric Fernández	CTTC
Anna Barra	CTTC		
Jose Navarro	CTTC		

## **REVIEW: CORE TEAM**

Reviewed by	Company	Date	Signature
Oriol Monserrat	CTTC	08/08/2019	

## 1 INTRODUCTION

This document contains a short description of the procedure to obtain the DInSAR based products in the Canary Island site and the obtained results: the displacement maps (DIM), the deformation activity maps (DAM) and the active deformation areas map (ADA). The DIM and DAM maps are directly derived from Sentinel-1 (S-1) data by means of A-DInSAR analysis; DIM is a map derived directly from the unwrapped interferogram, provides qualitative information and requires expert users. DAM map consists in the estimated velocity in mm/yr and the deformation time series (TS) for a set of selected points. It is relatively easy to be interpreted. Finally, the ADA map, is derived by a semi-automatic extraction of the most significant detected active deformation areas. It is a very simplified map that point the attention on the areas affected by displacements and provides key information about its movement.

Together with the document we deliver the final results obtained in the Canary Island test site. These results have been obtained after an iterative testing and assessment process done in collaboration with IGN and IGME teams in order to improve the deliveries and to tune the used approach. The quality of the obtained results is good enough in almost all the test site area. However, there are some issues to be solved in order to improve the coverage with a reasonable reliability. We have focused most of the tests on Hierro Island given that it was the most interesting island for civil protection. The main goal was to tune the approach. For this reason, we have worked with a short dataset easy to be reprocessed.

This document consists of 5 sections: after the introduction, Section 2 describes the Sentinel-1 dataset; Section 3 describes the procedure; Section 4 the format of the delivered maps; Section 5 the obtained results and finally Section 6 underline particular aspects about the results.

## 2 DATASET DESCRIPTION

The three measured islands, La Palma, Hierro and Tenerife, are covered by a single Sentinel-1 frame. The dataset consisted of 83 Sentinel-1 Wide Swath, covering one year and 8-month period, starting in January 2017 and ending in August 2018. Due to critical atmospheric components and noise, some images were discarded for different islands. In particular, the dataset of El Hierro island was reduced to 74 images covering the period from May 2017 to August 2018. La Palma dataset covered the same period but with 70 images. Table 2.1 show the acquisition dates of the used images. In Table 2.2, are shown the main characteristics of the used dataset.

To remove the topographic contribution, we have used the SRTM Digital Elevation Model provided by NASA, and the precise orbits provided by the European Space Agency (ESA). To derive the deformation maps, we have generated a network of 82 interferograms with a maximum temporal baseline of 12 days for Tenerife, 69 for La Palma with maximum temporal baseline of 12 days and 73 interferograms with maximum temporal baseline of 12 days for el Hierro Island.

The selected resolution has been the multi-look 2x10 that corresponds to a footprint of approximately 28x36 m. This resolution is a compromise between density of measureable points, due to coherence, and resolution high enough to detect small deformation phenomena.

Nº image	Date						
1	2017/01/08	22	2017/08/06	43	2017/12/22	64	2018/04/27
2	2017/01/20	23	2017/08/12	44	2017/12/28	65	2018/05/03
3	2017/02/01	24	2017/08/24	45	2018/01/03	66	2018/05/09
4	2017/02/13	25	2017/08/30	46	2018/01/09	67	2018/05/15
5	2017/02/25	26	2017/09/05	47	2018/01/15	68	2018/05/21
6	2017/03/09	27	2017/09/11	48	2018/01/21	69	2018/05/27
7	2017/04/02	28	2017/09/23	49	2018/01/27	70	2018/06/02
8	2017/04/14	29	2017/09/29	50	2018/02/02	71	2018/06/08
9	2017/04/26	30	2017/10/05	51	2018/02/08	72	2018/06/14
10	2017/05/20	31	2017/10/11	52	2018/02/14	73	2018/06/20
11	2017/05/26	32	2017/10/17	53	2018/02/20	74	2018/06/26
12	2017/06/01	33	2017/10/23	54	2018/02/26	75	2018/07/02
13	2017/06/07	34	2017/10/29	55	2018/03/04	76	2018/07/14
14	2017/06/13	35	2017/11/04	56	2018/03/10	77	2018/07/20
15	2017/06/25	36	2017/11/10	57	2018/03/16	78	2018/07/26
16	2017/07/01	37	2017/11/16	58	2018/03/22	79	2018/08/01
17	2017/07/07	38	2017/11/22	59	2018/03/28	80	2018/08/07
18	2017/07/13	39	2017/11/28	60	2018/04/03	81	2018/08/13
19	2017/07/19	40	2017/12/04	61	2018/04/09	82	2018/08/19
20	2017/07/25	41	2017/12/10	62	2018/04/15	83	2018/08/25
21	2017/07/31	42	2017/12/16	63	2018/04/21		

**Table 2-1 List of the Downloaded images. Grey cells are the el Hierro subset. Green numbers represent the set of images for La Palma.**

<i>Satellite</i>	Sentinel-1
<i>Acquisition mode</i>	Wide Swath
<i>Period</i>	Jan 2017 - March 2018
<i>Minimum revisit period [days]</i>	6
<i>Wavelength (<math>\lambda</math>) [cm]</i>	5.55
<i>Polarization</i>	VV
<i>Multi-look 2x10 resolution (azimuth/range) [m]</i>	28/36
<i>Orbit</i>	Ascending
<i>Incidence angle of the area of interest</i>	$\approx 32^\circ - 41.85^\circ$

**Table 2-2 Dataset summary.**

### 3 PROCEDURE DESCRIPTION

The S-1 data processing has been done by using and tuning the software tools developed by CTTC in the framework of the European Project Safety (<http://safety.cttc.cat/>). The used procedure has two main phases. In the first phase is calculated the stack of interferograms and

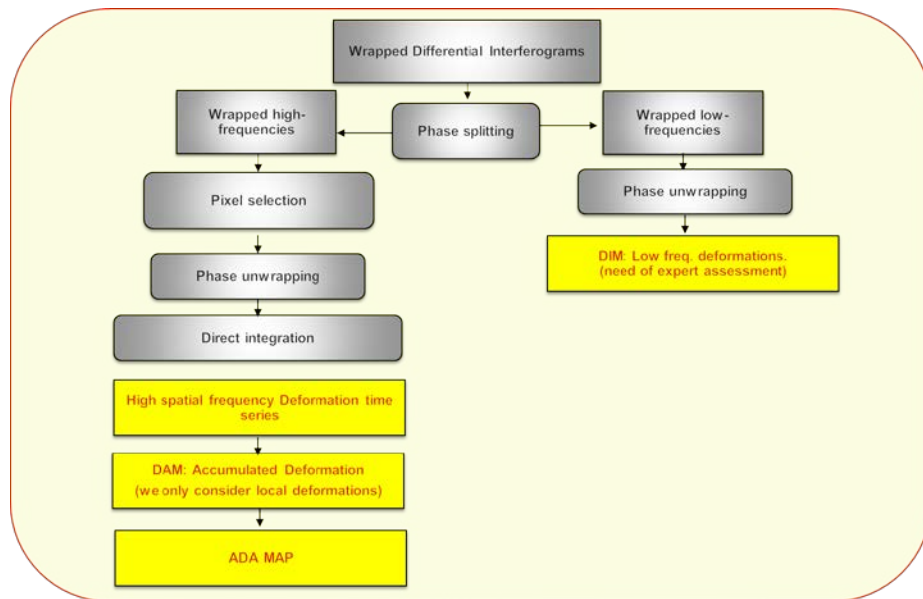


**Figure 3.1: Flow chart of the data processing**

coherences and in the second phase are generated the DIM and DAM maps. In the following lines are described the main steps of the procedure used for the Canary Island test site (see Figure 3.1).

The procedure is based in the direct integration of consecutive interferograms (see Barra et al. 2016). The main goal is to fully exploit the high coherent phase of the 6-day interferograms with two purposes: (i) to obtain a good coverage at regional scale and (ii) to be able to detect relatively fast displacements. The input of the procedure is a set of N images, the corresponding N-1 complex-interferograms formed by consecutive image pairs, and a Digital Elevation model. Here in advance are described the key steps to derive the maps.

### 3.1 Phase splitting

The phase splitting consists in the application of a space filtering to each interferogram to discriminate those signals that have a smooth phase changes in space (mainly atmospheric contribution) from those with higher space gradients (ground displacements or topographic errors). To do it, we propose to use the Butterworth filter ([Butterworth](#)). It is defined by the form:

$$G(\Omega) = \frac{1}{\sqrt{1 + \left(\frac{\Omega}{\Omega_c}\right)^{2N}}} \quad (1)$$

Where G is the gain,  $\Omega$  is the frequency,  $\Omega_c$  the cut-off frequency and N is the order.

The result is, for each wrapped interferogram, the so-called low frequency component and the residuals, here below named High frequency component (see Figure 3.2).

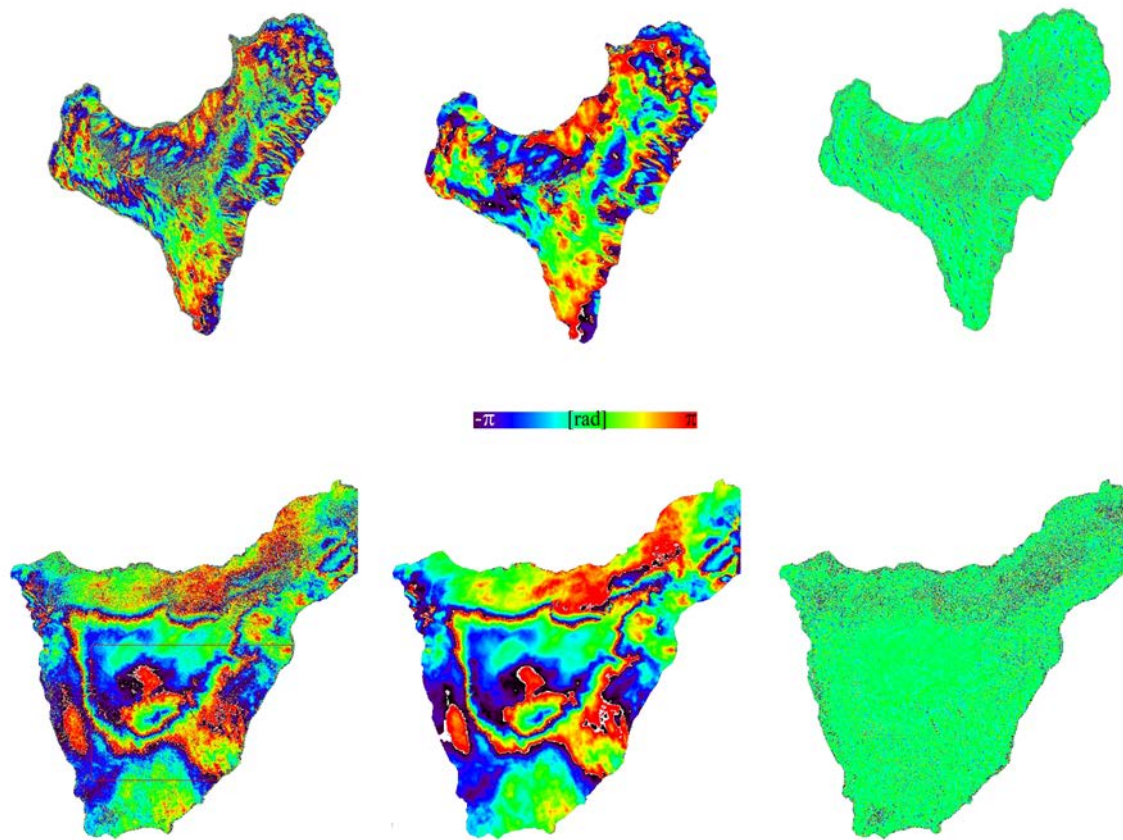


**Figure 3.2: Example of phase splitting. Left, original wrapped interferogram. Centre, Low frequencies. Right, residuals or high frequencies. Above, El Hierro island. Bottom, Tenerife.**

These two components are interpreted as follows:

- The low frequencies are assumed to be almost atmospheric contribution. However, it cannot be discarded potential fast movements with high spatial correlation. This aspect is commented later in this document.
- The high frequencies are residual phases containing only slow movements (few mm/yr to several cm/yr), fast local movements (few mm/day) and residual topographic errors due to the used DEM (see Crosetto et al 2011).

Here in advance the approach is split in two paths: the high frequency and the low frequency path.

### 3.2 DAM and ADA generation: High frequency path

In this process are generated the DAM and ADA maps. The first step is the pixel selection. In the Canary Island test site, we have used the coherence criterion (Crosetto et al., 2011). The used threshold has been set empirically in 0.1. This selection is based in an iterative process done once for each test site and aimed to select a trade-off between coverage and phase unwrapping quality.

The second step is the phase unwrapping. It is performed for each interferogram and over the set of selected pixels. The used approach is the Minimum Cost Flow method described in Constantini et al., 1999). Figure 3.3 show examples of phase unwrapping at both El Hierro and Tenerife island. It can be seen that the wrapped phases are almost flat and therefore, the phase unwrapping is not affected by critical errors.

The following step is the so called direct integration that is performed point wise and described by the following equation (2):

$$\left. \begin{array}{l} \varphi_n = \varphi_{n-1} + \Delta\varphi_{(n-1)n} \\ \varphi_0 = 0 \end{array} \right\} n = 0 \div N \quad (2)$$

Where  $\varphi_n$  is the accumulated phase at the acquisition time n,  $\varphi_{n-1}$  is the accumulated phase at the acquisition time n-1 and  $\Delta\varphi_{(n-1)n}$  is the unwrapped interferometric phase of the interferogram calculated using the images acquired at the times n-1 and n. Finally, the first image on time is set as 0.

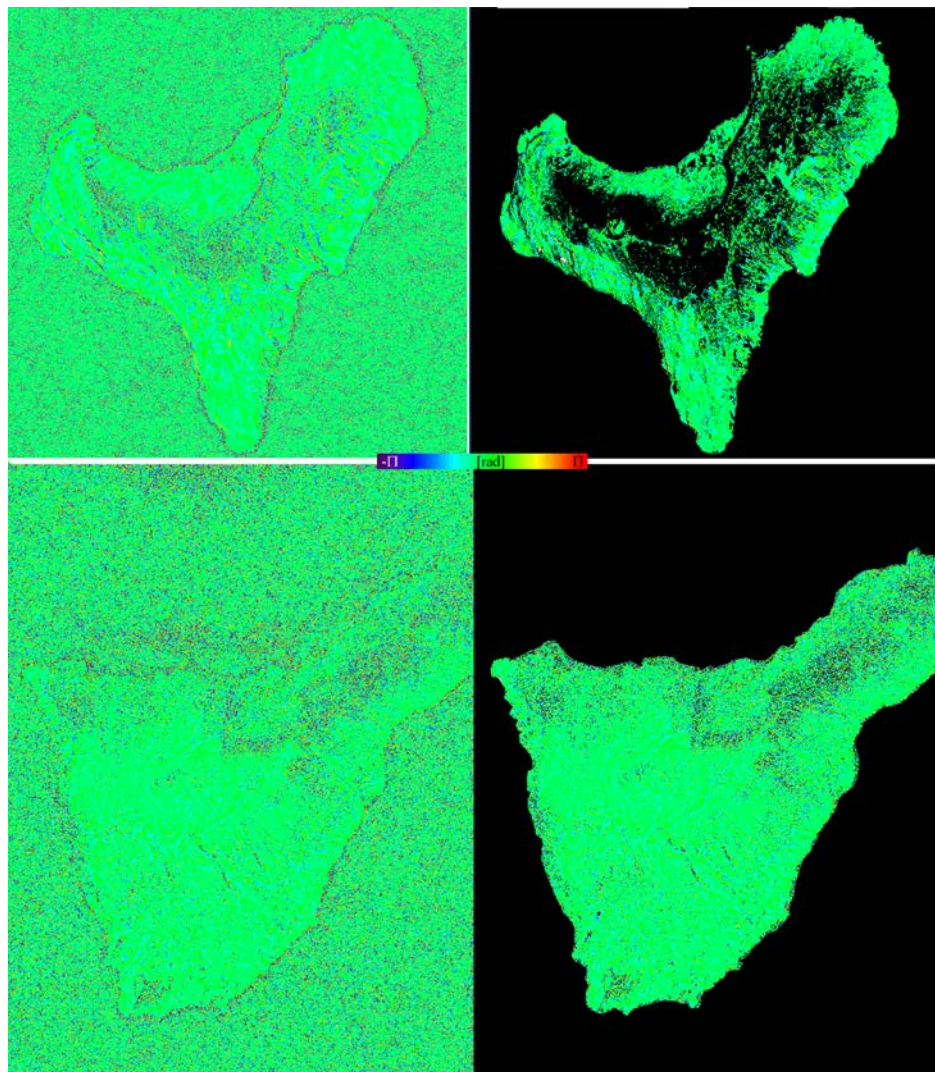


**Figure 3.3: Wrapped high frequency phase component (left) and the corresponding unwrapped phase (right). Hierro island (above) and Tenerife (below).**

The output of the direct integration is, for each point, the temporal evolution of the phase with respect the first acquisition time. Then after, this result is transformed to displacements by the following relation:

$$Disp_n = \frac{\varphi_n}{4\pi} \lambda \quad (3)$$

Where  $Disp_n$  is the accumulated displacement of the point at the acquisition time  $n$ ,  $\varphi_n$  is the accumulated phase (in radians) at the acquisition time  $n$  and  $\lambda$  is the wavelength of the satellite (56.6 mm for Sentinel-1). Finally, for each point, we perform the displacement velocity estimation. The final results are the  $N$  displacement maps (DAM) at the  $N$  acquisition times of the satellite. For each point we obtain the temporal evolution of the displacement and the velocity.

The last step is to geocode the DAM in order to obtain the ground coordinates of the measured points and to find the Active Deformation Areas (ADA) map. The ADA map has been generated by using the ADA finder app developed in the framework of the Safety (<http://safety.cttc.cat/>) and Mommit (<https://www.momit-project.eu/>) EU projects (Barra et al. 2017; Navarro et al. 2018).

### 3.2.1 Remarks on the used approach and issues to be solved

The results were compared with those obtained by using Persistent Scatterer (PS) technique (Crosetto et al 2016), a consolidated and reliable technique. The comparison was performed on a set of common points. The comparison results confirmed the reliability of the approach at least for this set points. For example, the standard deviation of the accumulated displacement differences is  $\approx 8$  mm and the average 1 mm. However, there were areas without PS, i.e. not included in the comparison, with uplift deformation trends where no movements were expected and difficult to be interpreted from a geological point of view. The explanation to these trends is the integration in time of a systematic error of the filtering in areas with low coherence. This problem is still not solved in a general way. However, for the Canary Island site, we exploited the high coherence at a relatively long temporal baselines to solve it. The used approach is: (i) select an interferogram with high coherence and at least one-year temporal baseline; (ii) split it to get the high frequency component. (iii) unwrap it; (iv) compare the result with the DAM map covering the same period; (iv) remove the areas with absolute differences bigger than 8 mm. Figure 3.4 shows the obtained DAM in El Hierro Island after applying the post-processing correction. It is worth noting that this solution is not applicable at every place. It is based in the coherence stability of the Canary Islands at relatively long temporal baselines.

## 3.3 DIM generation: Low frequency path

The DIM map is a deformation map derived from the low-frequency component of each interferogram. It is processed assuming that the low frequency phase component is due to displacement. The analysis of these maps is qualitative, requires user expertise and must be done with the support of complementary data like GPS or other geodetic techniques.

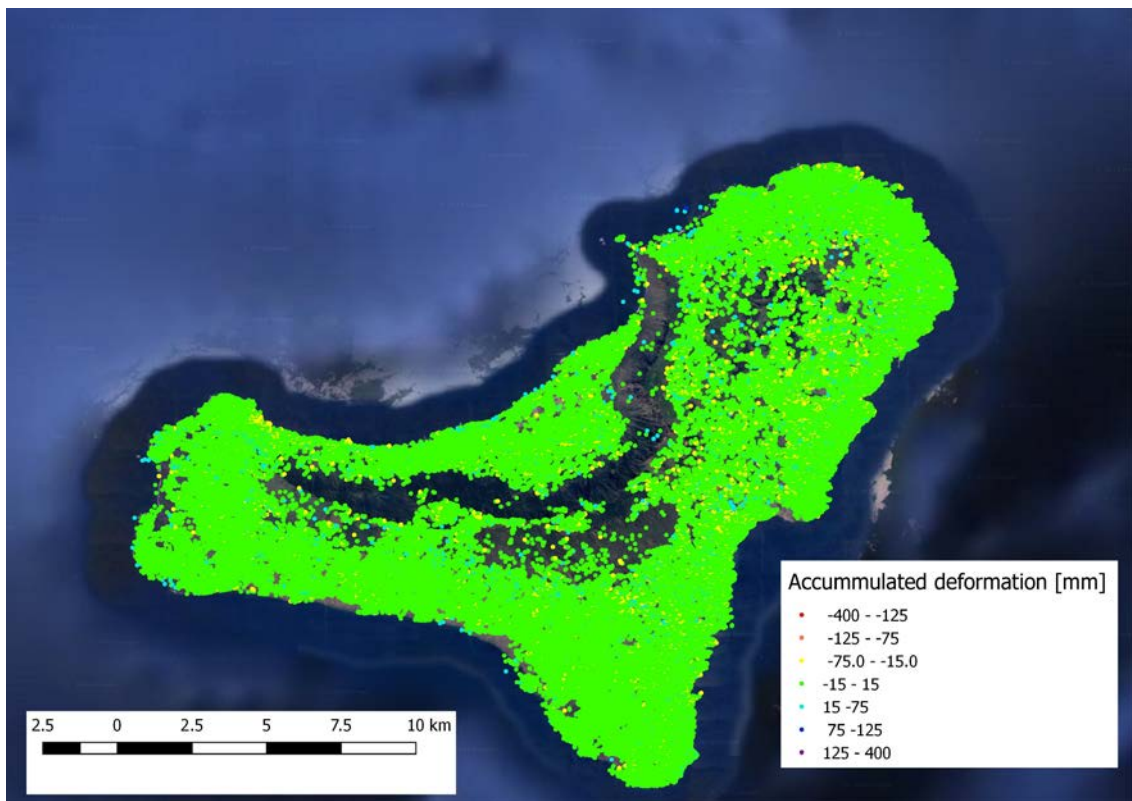


**Figure 3.4: Wrapped high frequency phase component (left) and the corresponding unwrapped phase (right). Hierro island (above) and Tenerife (below).**

For each interferogram, the approach is: (i) to perform the phase unwrapping; (ii) to estimate the corresponding displacements by using the equation (3); (iii) to interpret the results by integrating it with measurements coming from other techniques and if possible with other interferograms covering almost the same period. Figure 3.5 show and example of low-frequency-component and the corresponding DIM in radar geometry. In this example, all the signal is due to atmospheric effects.

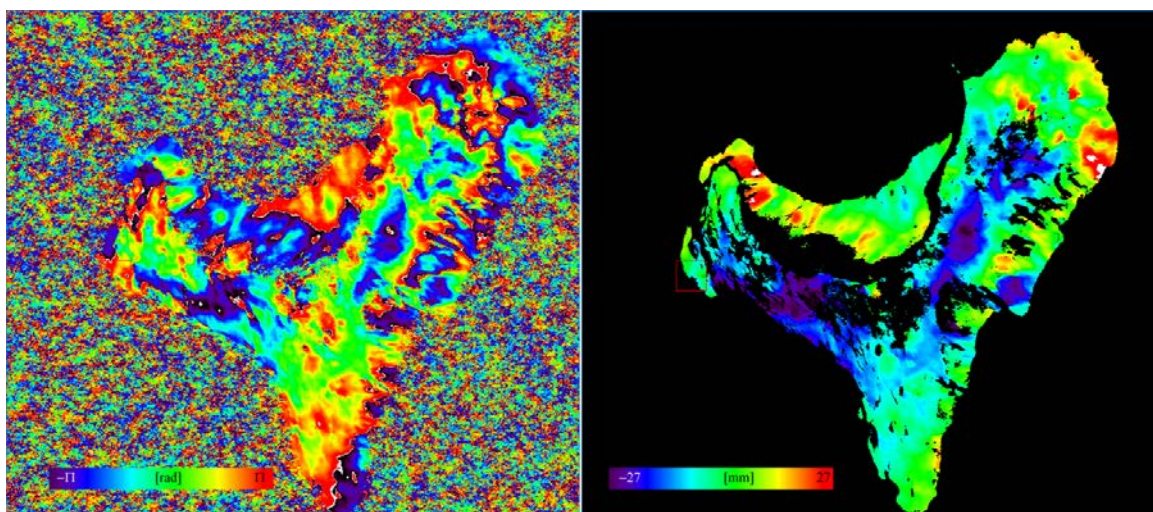


**Figure 3.5: 6-day wrapped low frequency phase component (left) and the corresponding DIM map (right) of el Hierro Island.**

## 4 MAP DELIVERY FORMAT

For each island have been delivered two shape files that represent the first version of the DAM and the ADA maps. The DIMs were produced and analyzed in radar geometry during the processing. There were not detected significant displacement signals in the DIMs during the monitored period.

The DAM and the ADA map represents the main goal of the task 3.3 Deformation activity maps. However, the ADA map has been also generated given that it can be also helpful to support early warning of long-term processes. It is an useful tool that eases the DAM analysis.

The DAM shape file fields are:

Field	Description	Units
<i>E</i>	UTM East	[m]
<i>N</i>	UTM North	[m]
<i>Lambda</i>	WGS84 Geographic Longitude	[°]
<i>Fi</i>	WGS84 Geographic Latitude	[°]
<i>ADA_ID</i>	ADA id. Containing the point [-1 if it is not active point]	
<i>Velocity</i>	Point displacement velocity	[mm/year]
<i>Def_mean</i>	Averaged deformation of the last 4 dates	[mm]
<i>H</i>	SRTM Height	[m]
<i>Etopo</i>	Topographic error (note that is set to zero)	[m]
<i>Daaaaammdd</i>	Deformation value at date aaaa/mm/dd	[mm]

The ADA shape file fields are:

Field	Description	Units
<i>ADA_ID</i>	Identity of the	
<i>NAPS</i>		
<i>X_MEAN</i>	UTM East	[m]
<i>Y_MEAN</i>	UTM North	[m]
<i>VEL_MIN</i>	WGS84 Geographic Longitude	[°]
<i>VEL_MAX</i>	WGS84 Geographic Latitude	[°]
<i>VEL_CLASS</i>	ADA id. Containing the point [-1 if it is not active point]	
<i>DEF_MEAN</i>	Point displacement velocity	[mm/year]
<i>TNI_CLASS</i>	Averaged deformation of the last 4 dates	[mm]
<i>SNI_CLASS</i>	SRTM Height	[m]
<i>QI_CLASS</i>	Topographic error (note that is set to zero)	[m]

## 5 OBTAINED RESULTS

Figure 5.1 shows the Tenerife DAM. The colours represent the accumulated deformation during the monitored period. The north east part of the island does not have points because it was not included in the acquisition frame. A total of 661544 points have been measured. The standard deviation of the velocity is 4.1 mm/yr. The moving threshold, i.e. the minimum velocity of a point to be considered a moving point, has been set as 8.2 mm/yr (i.e.  $2\sigma$ ). This threshold is relatively high. However, it is expected a significant decrease with longer monitoring periods. There have not been identified critical displacements during the monitored period.

Figure 5.2 show a detail of the ADA map. A total of 59 ADAs have been identified in Tenerife. 42 of the with QI 1, that means reliable (see Barra et al., 2017). Most of them are very small areas concentrated in slopes and probably due to sliding surficial materials. The high number is also a little bit misleading given that some of them could be part of a single movement area. The Figure 5.2 shows an area of Tenerife where can be seen ADAs with different QI. QI of 1, in green, representing a reliable ADA, QI of 3 in soft orange that are areas to be checked and QI of 4, in red, that are not reliable.

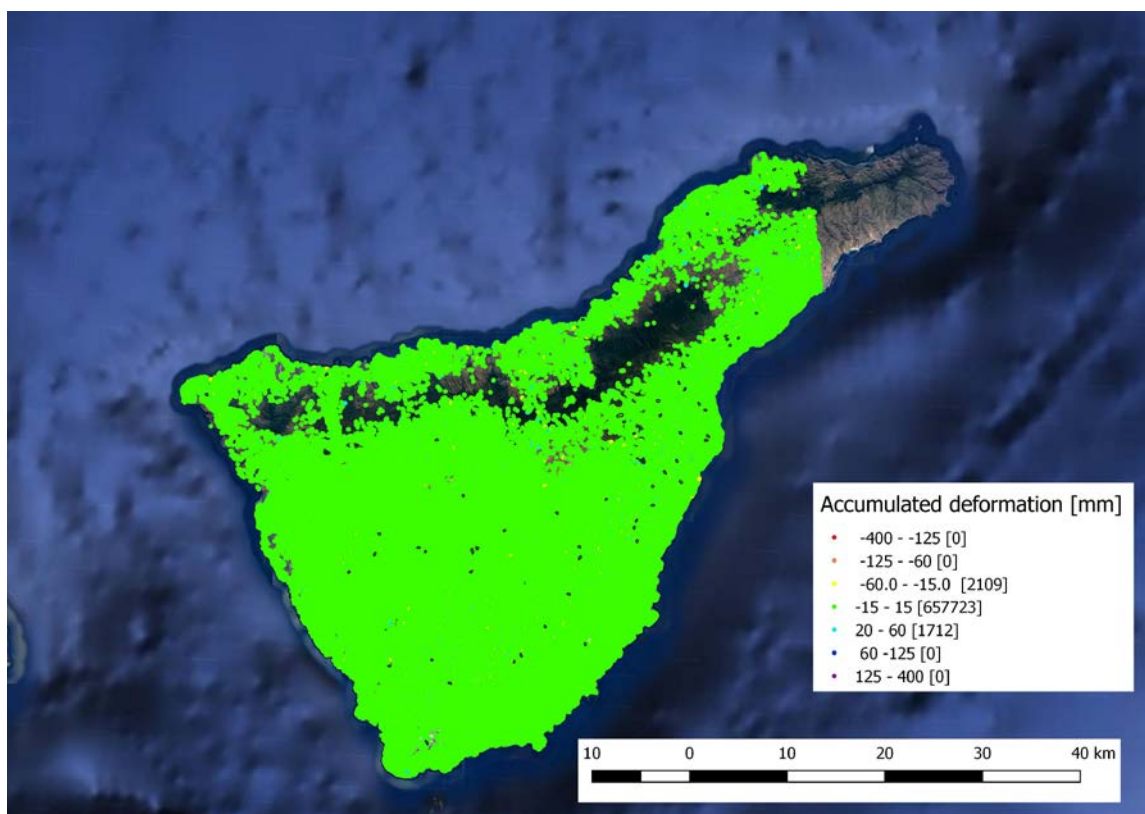


**Figure 5.1: DAM map of Tenerife representing the accumulated displacement in the monitored period.**



**Figure 5.2: ADA map in Tenerife.**

Figure 5.3 shows El Hierro DAM colour-coded also by the accumulated deformation during the monitored period. The number of measured points is 96196. The standard deviation of the velocity is 5.6 mm/yr and the moving threshold has been set as 11.2 mm/yr (i.e.  $2\sigma$ ). This threshold is higher than the Tenerife one mainly due to that we have used a shorter period. There have not been identified critical displacements during the monitored period.

Only 4 ADA have been identified. Most of them seem to be subsidence and uplift processes due to water exploitation. However, this is still a possibility that is under analysis. In Figure 5.4 are shown the 4 ADAs of el Hierro Island.

Finally, Figure 5.5 shows the DAM map of La Palma. 301109 points have been measured. The standard deviation of the velocity is 6.86 mm/yr. In this Island we have not detected any ADA.

## 6 OBSERVATIONS

- The total number of points is 1058849: 661544 in Tenerife, 301109 in La Palma and 96196 in Hierro.
- The deformations are in Line of Sight, i.e. they represent the projection of the real 3D displacement in the direction “satellite-point”.
- The negative values represent points that are going far from the satellite. The positive ones represent those moving towards the satellite.

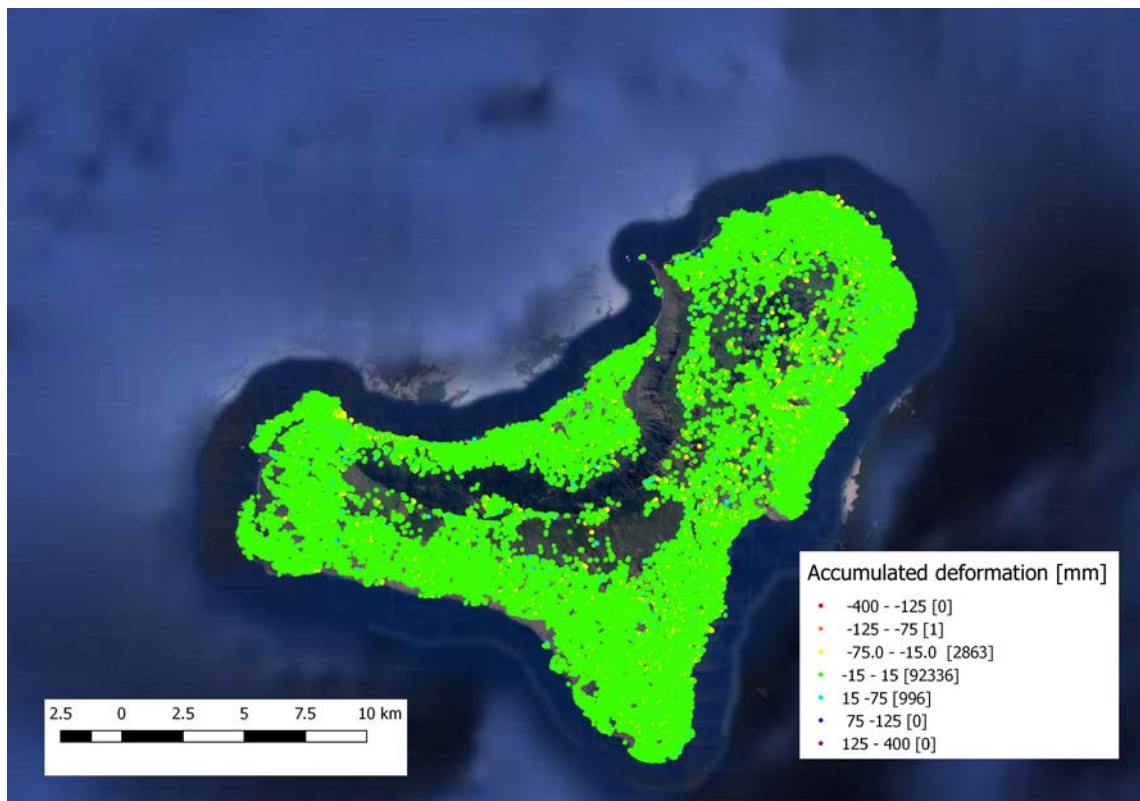


**Figure 5.3: DAM map of el Hierro representing the accumulated displacement in the monitored period.**



**Figure 5.4: ADA map of el Hierro.**

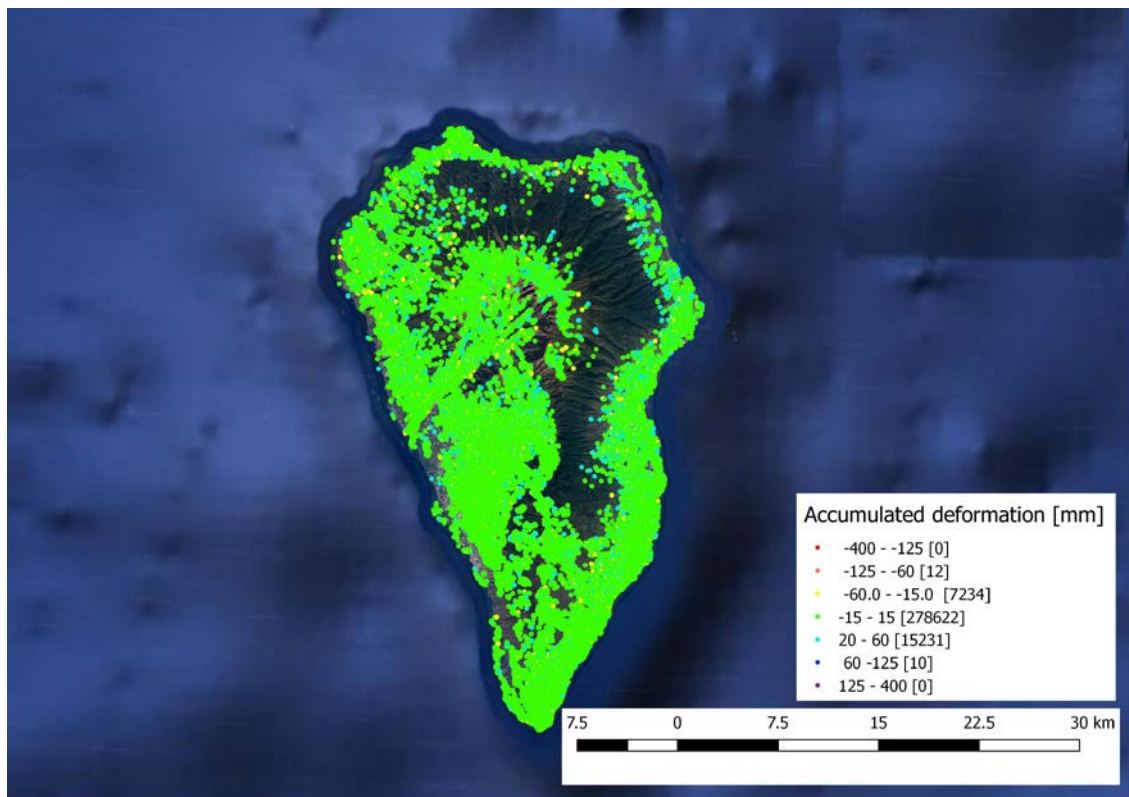


**Figure 5.5: DAM map of La Palma representing the accumulated displacement in the monitored period.**

- The activity thresholds are 8.2 mm/yr for Tenerife, 13.6 mm/yr for La Palma and 11.2 mm/yr for El Hierro. The reason of these high thresholds is that the monitored period is still short. It is expected a significant improvement with longer periods.
- Some active areas have been detected in Tenerife and El Hierro. However, these areas are not considered critical. The QI index seems to be a good indicator about the reliability of the detected active process.
- We suggest to use the activity thresholds of  $2\sigma$  (6.8 mm/yr) for the visualization of the delivered velocity map. In this way, you visualize only the most reliable deformation without losing PS velocity information in correspondence of deformation phenomena. For a local, detailed, visualization you can change the colour scale.
- As a general remark, the proposed approach seems to work and provides good results. However, as commented above in this document, there are still some aspects to be solved to make it replicable in different areas like, e.g., Valle di Aosta site.

## 7 REFERENCES

Barra, A., Solari, L., Béjar-Pizarro, M., Monserrat, O., Bianchini, S., Herrera, G. et al. (2017). A Methodology to Detect and Update Active Deformation Areas Based on Sentinel-1 SAR Images. *Remote Sensing*, 9(10), 1002.

Barra, A., Monserrat, O., Mazzanti, P., Esposito, C., Crosetto, M., & Scarascia Mugnozza, G. (2016). First insights on the potential of Sentinel-1 for landslides detection. *Geomatics, Natural Hazards and Risk*, 7(6), 1874-1883.

Costantini, M. (1998). A novel phase unwrapping method based on network programming. *IEEE Transactions on geoscience and remote sensing*, 36(3), 813-821.

Crosetto, M., Monserrat, O., Cuevas-González, M., Devanthéry, N., & Crippa, B. (2016). Persistent scatterer interferometry: a review. *ISPRS Journal of Photogrammetry and Remote Sensing*, 115, 78-89

Crosetto, M., Monserrat, O., Cuevas, M., & Crippa, B. (2011). Spaceborne differential SAR interferometry: Data analysis tools for deformation measurement. *Remote Sensing*, 3(2), 305-318.

Navarro, J. A., Cuevas-González, M., Barra, A., & Crosetto, M. Detection of Active Deformation Areas based on Sentinel-1 imagery: an efficient, fast and flexible implementation.